Monotopic and heteroditopic calix[4]arene receptors as hosts for pyridinium and viologen ion pairs: a solution and solid-state study†

Luca Pescatori,[a] Arturo Arduini,[a] Andrea Pochini,[a] Andrea Secchi,*[a] Chiara Massera[b] and Franco Ugozzoli[b]

Received 1st April 2009, Accepted 8th June 2009
First published as an Advance Article on the web 16th July 2009
DOI: 10.1039/b906409e

The binding efficiency of a series of monotopic (**1–2**) and heteroditopic (**3–4**) calix[4]arene-based receptors has been evaluated in chloroform solution toward *N*-methylpyridinium ion pairs using NMR and UV/vis spectroscopic techniques. These experiments provided evidence that, due to a positive cooperative effect, the presence of a phenylurea H-bond donor group on the upper rim of the calix[4]arene macrocycle increases the recognition abilities of the heteroditopic receptors by up to two orders of magnitude with respect to the monotopic receptors. The heteroditopic receptors are also able to form 2:1 host–guest inclusion complexes with dimethylviologen salts both in low polarity solvents and in the solid state. These complexes are stabilized through the cooperation of weak (CH–π and cation–π) and strong (hydrogen bonding) intramolecular interactions between the binding domains of the calix[4]arene host and the two ions of the guest ion pair.

Introduction

In recent years, considerable attention has been focused on the miniaturization of components to build up nanostructures endowed with specific functions.[1] The development of "nanoscale devices" can benefit the principles and methods of supramolecular chemistry.[2] Indeed, one can envision that the assembly of simple molecular components could lead to the fabrication of molecular devices capable of performing specific functions upon the application of external stimuli.

Calix[*n*]arenes[3] have been widely used in supramolecular chemistry as tridimensional receptors able to bind ion pairs in low polarity solvents.[4] In this context, we have reported that calix[*n*]arene derivatives functionalized on the macrocycle upper rim with hydrogen bond donor groups can be used as receptors for ion-pairs. In particular, triphenylureido calix[6]arenes have been employed as active components for the preparation of molecular machine prototypes, giving rise with *N*,*N*′-dialkyl-4,4′-dipyridinium salts to very stable and electrochemically reversible pseudorotaxane complexes.[5] In the calix[4]arene series, the binding abilities of the aromatic cavities of highly preorganised monotopic[6] and heteroditopic[7] calix[4]arene derivatives toward a series of tetramethylammonium (TMA) ion pairs characterised by counteranions of different coordination strengths were investigated. In these studies, the positive cooperative action[4b,8] of two complementary binding domains on ion-pair recognition was evidenced, for instance, by comparing the binding efficiency of the monotopic calix[4]arene-biscrown-3 (**1**) with its heteroditopic counterpart (**3**) having an ancillary hydrogen bond donor group on the same scaffold (see Fig. 1).[7b]

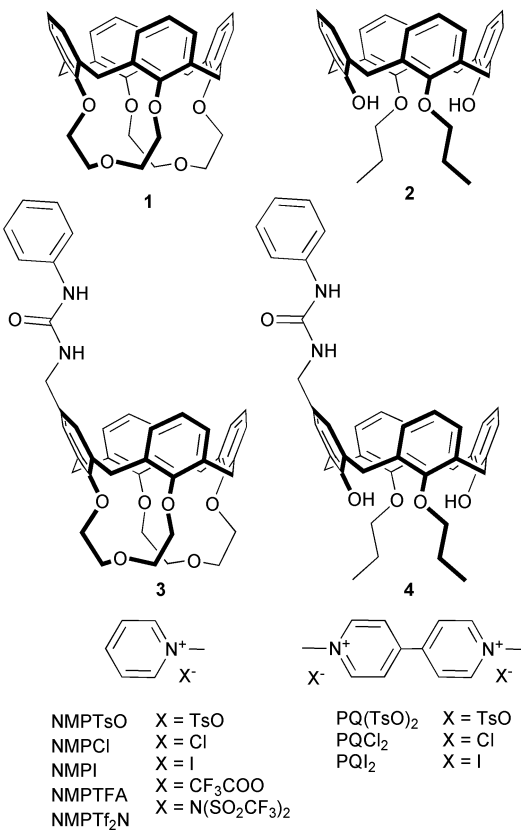

Fig. 1 Structural formulae of the calix[4]arene-based receptors (**1–4**) and of the *N*-methylpyridinium and *N*,*N*′-dimethylviologen salts used in the present study.

[a]*Dipartimento di Chimica Organica e Industriale and Unità INSTM, Sez. 4 – UdR Parma, Università degli Studi di Parma, via G.P. Usberti 17/a, I-43100, Parma, Italy. E-mail: andrea.secchi@unipr.it; Fax: +39 0521 905472; Tel: +39 0521 905409*

[b]*Dipartimento di Chimica Generale ed Inorganica, Chimica Analitica e Chimica Fisica, Università degli Studi di Parma, via G.P. Usberti 17/a, I-43100, Parma, Italy*

† Electronic supplementary information (ESI) available: Conformational parameters and CIF files for the solid-state structures of **1** ⊃ NMPI and **4**$_2$ ⊃ PQ(TsO)$_2$ inclusion complexes; Full 2D NOESY spectra of the mixture between **1** and NMPI and **3** and NMPCl in $CDCl_3$; 2D COSY, HMQC, ROESY and DOSY spectra of the 2:1 mixture between **4** and PQ(TsO)$_2$ in $CDCl_3$. CCDC reference numbers 725833 and 725834. For ESI and crystallographic data in CIF or other electronic format see DOI: 10.1039/b906409e

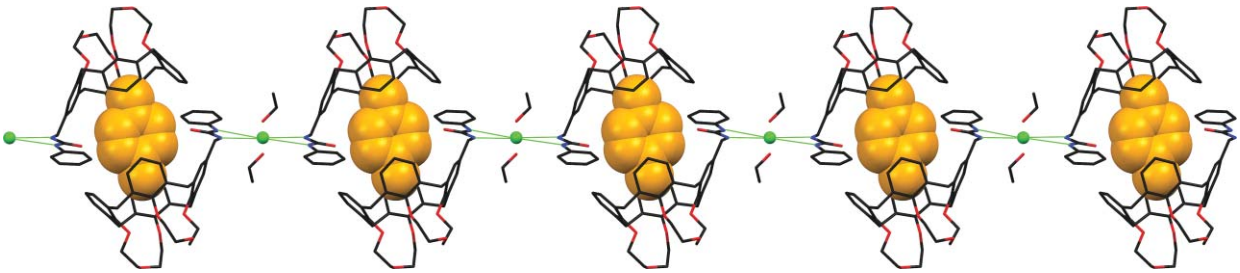

Fig. 2 Partial view of an infinite hydrogen-bonded 1D polymeric chain of self-assembled 2:1 complexes between heteroditopic calix[4]arene **3** and *N*-methylpyridinium choloride ion pairs (the disordered cationic guest is represented with CPK spheres, hydrogen atoms are omitted for clarity).[9]

We have recently used the binding ability of **3** for the construction of extended superstructures in the solid state with *N*-methylpyridinium chloride ion pairs (see Fig. 2).[9] In these self-assembled capsules, the pyridinium cation interacts with the two calix[4]arene units through CH–π[10] and cation–π interactions,[11] while the anion acts as bridging unit between the dimeric capsules through hydrogen bonding.

The transfer of the chemical information stored in this system for the development of more complex switchable functional devices, such as supramolecular polymers and intelligent materials,[12] should be based on a deeper understanding of the supramolecular interactions that stabilise these complexes. This aspect is particularly important in those cases where either the cation or the anion have a non-isotropic charge distribution, thus adding a further element of complexity to the system. Herein we report a systematic investigation of the parameters that affect the recognition of *N*-methylpyridinium and *N*,*N*′-dimethylviologen salts by calix[4]arene-based receptors in low polarity solvents[13] and in the solid state, by looking at both the structure of the host (preorganization and binding topicity) and the nature of the guest (charge effect and anion coordinating strength).

Results and discussion

Recognition of *N*-methylpyridinium ion pairs (NMPX)

Solution studies. The binding properties of monotopic calix[4]arenes **1–2** toward the series of *N*-methylpyridinium salts (NMPX) depicted in Fig. 1 were investigated by ^{1}H NMR spectroscopy[14] in $CDCl_3$ solution at 300 K. The set of salts was selected on the basis of the different coordinating character of the anion X.[15,16]

In a typical ^{1}H NMR titration experiment, increasing amounts of a solution of the calix[4]arene receptor (usually $c = 1.5 \times 10^{-2}$ M) were added to a solution of the NMPX salt (usually $c = 1.5 \times 10^{-3}$ M). After each addition, the variation of chemical shift experienced by the proton signals of the *N*-methylpyridinium (NMP) cation was monitored and plotted against the receptor–salt concentration ratio. The titrations carried out using the monotopic receptors **1** and **2** always showed time-averaged signals for the free and complexed species. As a typical example, we report in Fig. 3 the binding isotherms obtained during the titration of NMPI with **1**. The plots show that the aromatic cavity of **1** exerts an anisotropic shielding effect on the protons of the NMP cation, resulting in an extensive upfield shift of the corresponding resonances. After having verified the formation of 1:1 receptor–salt adducts through

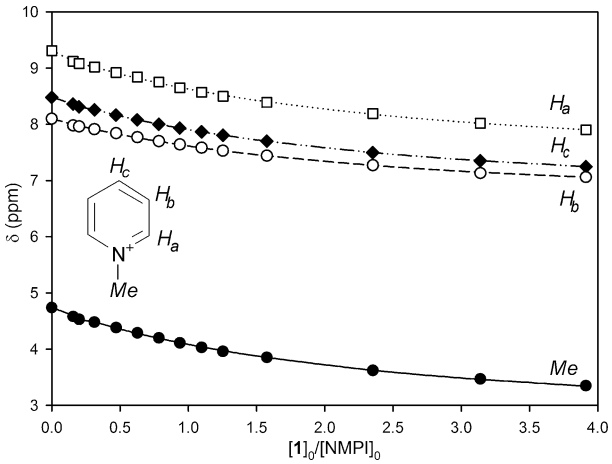

Fig. 3 Binding isotherms for the complexation of NMPI ($c = 1.3 \times 10^{-3}$ M) with **1** ($c = 10^{-2}$ M) in $CDCl_3$. Symbols ●, □, ○ and ◆ show the chemical shift variation of protons *Me*, H_a, H_b and H_c, respectively (see inset sketch).

the application of continuous variation methods (Job plot),[17] the apparent binding constants (log*K*) and the limiting upfield shifts ($\Delta\delta_\infty$, ppm) were calculated through the non-linear fitting[18] of the chemical shift variation experienced, upon complexation, by the NMP resonances (see Experimental).

The log*K* values gathered in Table 1 show that the binding efficiency of **1** increases as the coordinating strength of the anion decreases (see also Fig. 4a). The less coordinating bistriflimide (Tf_2N) and trifluoroacetate (TFA) counteranions afforded the highest log*K* value, while the more coordinating *p*-toluensulfonate (TsO) yielded the lowest log*K*.. With NMPI and NMPCl ion pairs, the inverse correlation between binding efficiency and coordinating strength of the anion was satisfied only when log*K* was calculated considering the chemical shift variation of the NMP methyl group (see Table 1 and Fig. 4a). In particular, with NMPCl a significant deviation from this general trend was observed (see Fig. 4a). Such behaviour can be tentatively explained considering that 1:1 binding stoichiometry could be affected by other factors.[19]

The analysis of the calculated limiting upfield shifts (see $-\Delta\delta_\infty$ values in Table 1) reveals that the binding mode of **1** is significantly affected by the strength of the ion pair. Indeed, the rigid "pseudo-*cone*" aromatic cavity[6b,20] of this receptor is able to recognise the NMPX ion pair either through the methyl group (*Me*) or the aromatic protons H_b and H_c of the NMP cation. However, $NMPTf_2N$, being the more "loose" ion pair among those investigated, is preferentially recognised through the acidic

Table 1 Binding constants (log$K$) and limiting upfield shifts ($\Delta\delta_\infty$, ppm) for the formation of 1:1 adducts of *N*-methylpyridinium salts with monotopic calix[4]arene receptors **1** and **2**[a,b]

		NMPTsO		NMPCl		NMPI		NMPTFA		NMPTf$_2$N	
Receptor	Resonance[c]	log$K$	$-\Delta\delta_\infty$	log$K$	$-\Delta\delta_\infty$	log$K$	$-\Delta\delta_\infty$	log$K$	$-\Delta\delta_\infty$	log$K$	$-\Delta\delta_\infty$
1	*Me*	2.06(2)[d]	1.8	2.38(5)	1.9	2.62(2)[d]	2.5	2.75(1)	1.8	2.94(3)	2.7
	H_a	2.06(3)	2.3	2.53(8)	2.1	2.71(5)	2.3	2.72(1)	2.2	2.95(1)	2.2
	H_b	1.99(3)	2.2	2.79(5)	1.5	2.55(3)	2.1	2.73(1)	2	2.92(1)	1.7
	H_c	2.00(4)	2.8	2.74(4)	1.9	2.56(3)	2.4	2.69(1)	2.4	2.93(1)	2
2	*Me*	2.11(9)	1.8	2.99(1)	1.1	3.35(4)	1.1	3.08(4)	1.1	3.02(1)	1.4
	H_a	2.48(1)	2.7	2.99(7)	2.4	3.44(6)	2.1	3.02(3)	2.2	2.98(1)	2.5
	H_b	2.34(5)	3.2	3.05(1)	2.4	3.33(5)	2.2	3.03(4)	2.4	3.02(2)	2.4
	H_c	2.54(5)	3	[e]	[e]	[e]	[e]	[e]	[e]	2.95(2)	3.1

[a] Determined by ^{1}H NMR spectroscopic titrations at $T = 300$ K in $CDCl_3$ (standard deviations in parentheses). [b] $\Delta\delta_\infty = \delta_\infty - \delta_{free}$ where δ_{free} (ppm): NMPTsO, 4.63 (*Me*), 9.21 (H_a), 7.97 (H_b), 8.36 (H_c); NMPCl, 4.83 (*Me*), 9.53 (H_a), 8.06 (H_b), 8.44 (H_c); NMPI, 4.74 (*Me*), 9.31 (H_a), 8.10 (H_b), 8.48 (H_c); NMPTFA, 4.68 (*Me*), 9.29 (H_a), 8.04 (H_b), 8.42 (H_c); NMPTf$_2$N, 4.52 (*Me*), 8.77 (H_a), 8.07 (H_b), 8.49 (H_c). [c] Resonance of the NMP cation used for the non-linear fitting (see Fig. 3 for labelling). [d] See ref. 6a. [e] Extensive overlapping of the resonances.

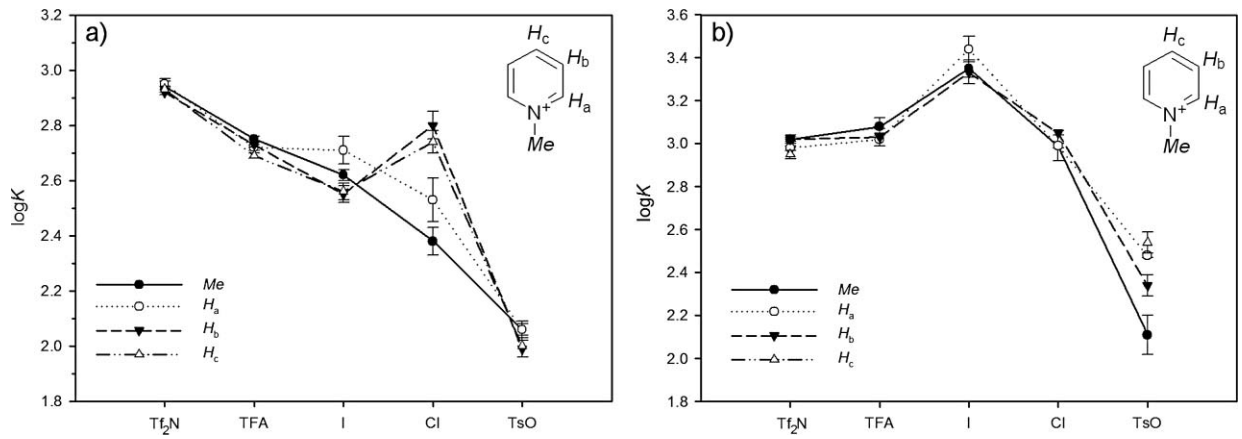

Fig. 4 Diagrams showing the log$K$ calculated through the non-linear fitting of the chemical shift variation endured by each NMP resonance upon complexation with receptors a) **1** and b) **2** respectively.

methyl group of its NMP cation ($-\Delta\delta_\infty$ for *Me* and H_c is 2.7 and 2 ppm, respectively), while the "tight" and more sterically demanding NMPTsO is likely bound through the electron poor aromatic moiety of its cation ($-\Delta\delta_\infty$ for *Me* and H_c is 1.8 and 2.8 ppm, respectively).

Receptor **2** is always a more efficient receptor than **1**; however, its binding efficiency cannot be correlated with the coordinating strength of the counteranion (see Fig. 4b). This receptor experiences its largest affinity for NMPI, that represents the ion pair characterised by the more polarisable anion. With the exception of NMPTsO, the log$K$ calculated for the other salts were all similar (see Table 1 and Fig. 4b).

The titration experiments involving **2** evidenced an extensive upfield shifts of the aromatic protons of the NMP cation. The $-\Delta\delta_\infty$ values calculated for these resonances were always larger than those calculated for the methyl group (see Table 1). These findings suggest that **2**, whose aromatic cavity can adopt a "flattened *cone*" conformation,[21] recognises preferentially the electron poor aromatic portion of the NMP cation probably *via* π–π stacking interactions.[22] The higher binding efficiency observed for **2** with respect to **1** can be thus reasonably ascribed to the better conformational adaptability[23] of its aromatic cavity that can maximise the interactions with the NMP cation regardless of the steric requirements imposed by the nature of the counteranion.‡

The binding properties of the heteroditopic receptors **3**[24] and **4**[25] (see Fig. 1) were initially investigated through ^{1}H NMR spectroscopic titrations. However, upon complexation, an extensive upfield shift and broadening of the resonances of the NMP cation was observed. Similarly, the resonances of the phenylurea NH protons of the calixarene receptor underwent a large downfield shift. Both findings suggested that, as found in the solid state,[9] ion-pair binding mainly occurs through the cooperation of a "soft" cation–π and a "hard" H-bond interaction. The former of these interactions occurs between the NMP cation and the π-rich aromatic cavity of the calixarene scaffold, while the stronger H-bond operates between the phenylurea group and the anion.

The broadening of the NMP resonances was unfortunately observed at the initial stages of the titrations. Such a

‡ The free phenolic groups of **2** can potentially interact with the counteranion through hydrogen bonding. The establishment of such interactions in solution of low polarity solvents was not observed with the NMPX salts, since the downfield shift experienced by the OH resonances during all the NMR titrations was negligible. Indeed, it is known that the OH groups are involved in intramolecular hydrogen bonding with the adjacent alkylated ones.

Table 2 Binding constants (log$K$) for the formation in $CHCl_3$ ($T = 300$ K) of 1:1 adducts between *N*-methylpyridinium salts (NMPX) and heteroditopic calix[4]arene receptors **3** and **4**[a,b]

Receptor	NMPTsO	NMPCl	NMPI	NMPTFA	NMPTf$_2$N
3	4.1(0.1)	5.5(0.2)	5.0(0.1)	5.0(0.1)	3.8(0.1)
4	4.75(0.07)	4.8(0.1)	5.0(0.2)	4.9(0.1)	3.5(0.1)

[a] Measured with UV/vis titrations (standard deviations in parentheses). [b] Spectral data λ_{max} (nm) and ε ($\times 10^3$ mol^{-1} L cm^{-1}) for the NMPX salts: 260, 4.1 (TsO); 260, 2.5 (Cl); 294, 2.9 and 376, 1.9 (I); 260, 4.1 (TFA); 260, 4.5 (Tf$_2$N); and for the free receptors: 273, 4.4 (**3**); 282, 7.8 (**4**).

phenomenon, consistent either with binding saturation or slow binding equilibria,[18] usually prevents the determination of reliable binding constants *via* NMR measurements. Therefore, the binding properties of **3** and **4** were investigated using more diluted solution of NMPX salts by UV/vis spectroscopy. In a typical titration experiment, increasing amounts of a 10^{-3} M solution of the receptor in $CHCl_3$ were added to a 10^{-4} M solution of the investigated NMPX salt in the same solvent. The titration of NMPI offered the most interesting results since the addition of the solution of **3** or **4** induced a blue-shift of the two low-energy charge-transfer (C.T.) bands, centred at $\lambda = 294$ and 367 nm, that are characteristic for the solutions of this salt in halogenated solvents.[26] The hypsochromic shift of the NMPI bands generates an isosbestic point at $\lambda = 293$ nm (see Fig. 5) and at $\lambda = 305$ nm with **3** and **4**, respectively. These shifts were reasonably ascribed to a reduction of the charge transfer process within the ion pair as a consequence of complex formation. This phenomenon was not monitored during the titrations of the other NMPX salts because in chloroform solution their C.T. bands are completely hidden by the strong absorption band of the pyridinium cation centred at $\lambda = 260$ nm. The families of spectra collected during the titrations were analysed with the Specfit/32 software.[27] The application of a 1:1 binding stoichiometry to the non-linear fitting of the spectral data yielded binding constants (log$K$) characterised by satisfactory standard deviations (see Table 2).

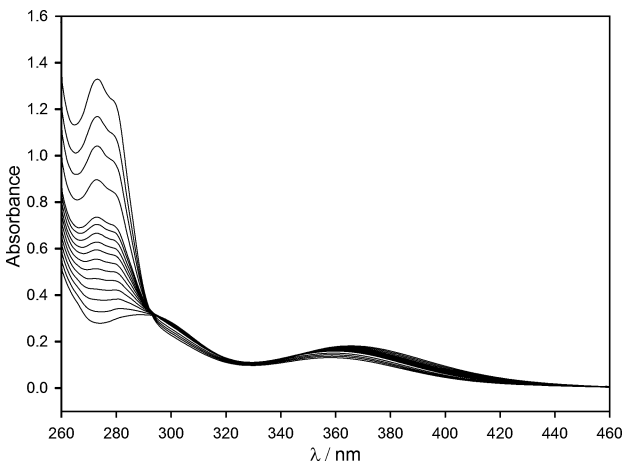

Fig. 5 Family of spectra collected for the titration of NMPI ($c = 1 \times 10^{-4}$ M) with **3** ($c = 1 \times 10^{-3}$ M) in $CHCl_3$.

The comparison of the binding constants calculated for **3** and **4** with those calculated for the corresponding monotopic receptors **1** and **2** (see Table 1), shows that the introduction of the ancillary anion binding site on the calix[4]arene cavity increases the affinity for the NMPX salts up to two orders of magnitude. Such binding enhancement has been tentatively evaluated in terms of a *cooperative heteroditopic effect*. The latter was expressed as the ratio between the binding constants calculated for each couple of heteroditopic and monotopic receptors having the same calix[4]arene skeleton.§ For the pair of biscrown-3-based receptors **3** and **1** the approximated ratios were 100 (TsO), 1300 (Cl), 240 (I), 170 (TFA), and 6 (Tf$_2$N). The highest increment was observed for NMPCl. The *cooperative effect* calculated for the couple of 1,3-dipropoxy calix[4]arene-based receptors **2** and **4** was 440 (TsO), 65 (Cl), 45 (I), 90 (TFA), and 2.5 (Tf$_2$N). For these more flexible receptors, the largest binding enhancement was recorded with the tight NMPTsO ion pair.

The binding data also show that, differently from the monotopic receptors, the binding efficiency of **3** and **4** cannot be directly correlated with the coordinating strength of the anion. In particular, the log$K$ values calculated for **4** were, within the experimental errors, almost identical with the exception of the poorly recognised NMPTf$_2$N "loose" ion pair. The more rigid and preorganised cavity of **3** determines a better binding selectivity. This receptor indeed maximises its recognition properties toward NMPCl (log$K = 5.5$), while its efficiency substantially drops (more than an order of magnitude) with the ion pairs of the series having the strongest (TsO) and the weakest (Tf$_2$N) coordinating anion. This behaviour can be rationalised by neglecting, in a first approximation, any entropic effect and assuming that the maximum recognition efficiency would mainly derive from the balance of two opposing effects: a) an energetic gain achieved by the interaction of the two ions with the two binding sites, and b) an energetic loss due to the stereochemical requirements associated with the recognition of tight ion pairs. In particular, specific steric requirements are involved in the pyridinium–anion and urea–anion interaction, and the latter is strongly dependent on the receptor structure. On this premise, the low efficiency recorded with NMPTsO by **4** (log$K = 4.75$) and in larger proportion by **3** (log$K = 4.1$), which is more rigid, can be ascribed to the latter adverse effect. On the other hand, the poor coordinating character of the Tf$_2$N anion should reduce the establishment of energetic H-bonding interactions with the phenylurea group of the receptors (effect a). The good affinity observed between NMPCl and **3** can be mainly ascribed to the small spherical anion that improves the fitting between the ion pair and the geometric arrangement of the two binding sites present in **3**.

The structure of the complexes in solution was inferred using 2D NMR techniques. A 2:1 mixture of **1** and NMPI was submitted to 2D NOESY and ROESY experiments. Two intense NOE cross-peaks in the NOESY spectrum evidenced the close proximity of the NMP methyl group to the aromatic protons H_m and H_p of the calix[4]arene skeleton (see Fig. 6a and ESI†).

Weak cross-peaks are also present between the proton H_a of NMP and the protons H_m and H_p of **1** (see ESI†), thus confirming that, as seen through the comparison of $\Delta\delta_\infty$ of Table 1, the NMP guest can interact with the cavity of the receptor also through its

§ The binding constant calculated monitoring the chemical shift variation experienced by the methyl group of the NMP cation were considered for the determination of the heteroditopic cooperative effect.

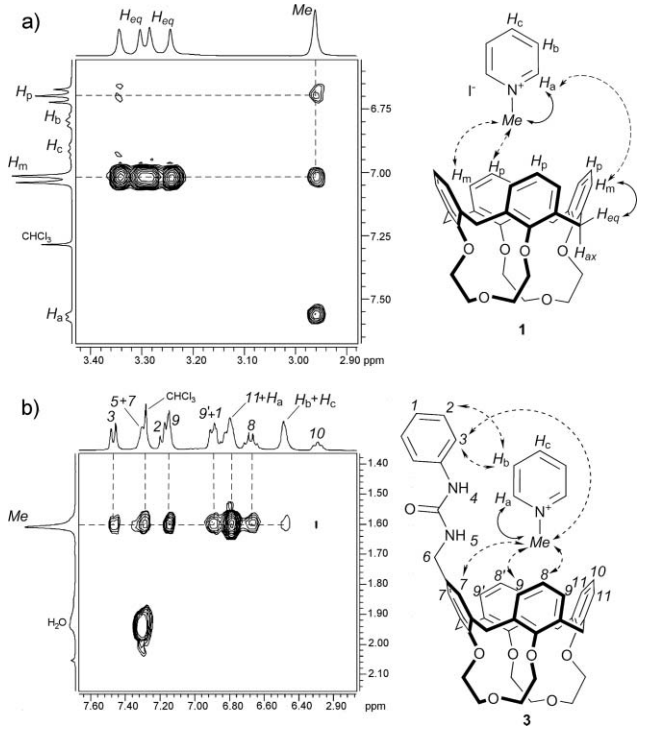

Fig. 6 Partial 2D NOESY spectra ($CDCl_3$, T = 300 K, mixing time = 0.4 ms) of a) 2:1 mixture of **1** and NMPI and b) 1:1 mixture of **3** and NMPCl (see ESI for full spectra†). The most representative NOE cross-peaks have been indicated in the spectrum with dashed lines. The relative intermolecular connections have been indicated in the schematic representation of the complex (not scaled) with dashed arrows.

aromatic moiety. Similar NOE correlations were present in the 2D NOESY spectrum of the mixture between **3** and NMPCl. Rather intense NOE cross-peaks arising between the aromatic protons H_b of the pyridinium ring and protons 2 and 3 of the phenylurea moiety (see Fig. 6b and ESI†) were also found, suggesting the proximity of these two aromatic rings.

Solid-state studies. Crystals suitable for X-ray analysis were obtained from the evaporation of an equimolar mixture of **1** and NMPI in chloroform. The crystal structure revealed the formation in the solid state of an inclusion complex (**1**⊃NMPI) in which the cavity of **1** is filled with the methyl group of the NMP cation (see Fig. 7a). The aromatic cavity, which usually adopts a pseudo-C_4 symmetry,[21] is forced by the complexation into a pseudo-C_2 elliptical *cone* conformation, as shown by the conformational parameters ϕ and χ (see ESI†).[28] The attraction between the CH_3 group and the three aromatic rings A, D and C of **1** is driven by three CH–π interactions.[10] The geometric parameters of these interactions show that the strongest attractions occur with the two opposite phenolic rings A and C, which show the shortest C···Ct (centroid) distances, whereas the interaction with the phenolic ring D is weaker (see Table 3) due to the higher value of its δ angle (opposed rings D and B diverge more than A and C; see ESI†).

The iodide ion is segregated outside the cavity of **1** and shielded from strong interactions with the NMP cation: the shortest I···C_{NMP} distance is 3.97 Å and it is close to the sum of the van der Waals radii of C (1.7 Å) and I^- (2.2 Å).[29] In the symmetry-extended structure, the **1**⊃NMP cationic complexes and the

Table 3 Geometric parameters relating to the CH–π and hydrogen bond interactions found in the **1**⊃NMPI complex.[a]

Interaction	Distance (Å)		Angle (°)
Donor–H···Acceptor	H···*A*	*D*···*A*	*D*–H···*A*
C(1G)–H···Ct(A)	2.44	3.44(1)	174
C(1G)–H···Ct(C)	2.72	3.35(1)	122
C(1G)–H···Ct(D)	2.82	3.70(1)	156

[a] Ct indicates the centroids of the calix[4]arene aromatic rings.

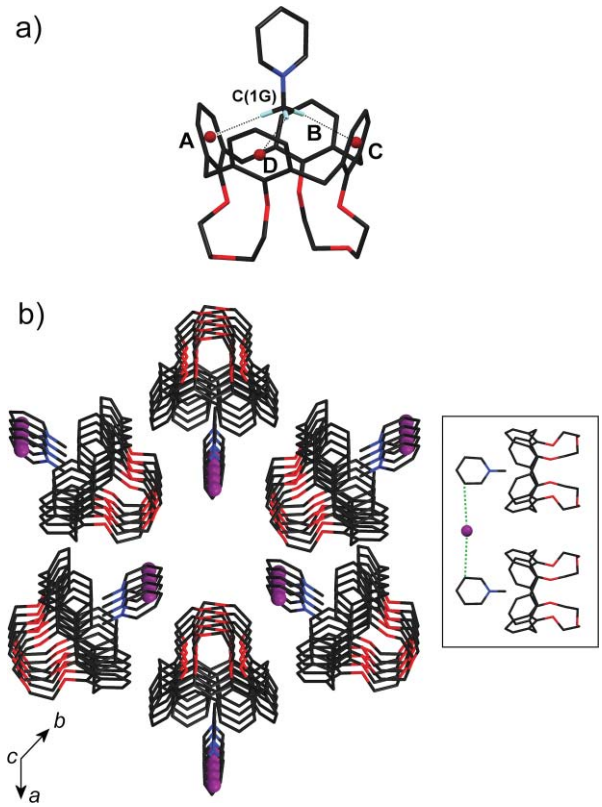

Fig. 7 Perspective stick view of a) the crystal structure of the **1**⊃NMP cationic complex and of b) the self-assembled **1**⊃NMPI complexes along the *c* crystallographic axis (in the inset the superstructure is viewed orthogonal to the *c* crystallographic axis).

iodide anions self-assemble in clusters of six **1**⊃NMPI units in a columnar arrangement, running along the crystallographic *c* axis, with a three-fold symmetry. The iodide anions are interdigitated between the cationic complexes along the same crystallographic axis (see Fig. 7b). The crystalline structure of **1**⊃NMPI is thus the result of the cooperation between weak and strong intermolecular interactions: the weak, but directional, CH–π interactions are responsible of the complexation of the NMP cation within the calixarene cavity, and the strong, but not directional, electrostatic interactions are the structure-directing factor for the self-assembly of the cationic complexes **1**⊃NMP^+ and the iodide anions in the crystal lattice.

Recognition of dimethylviologen ion pairs

The binding properties of the heteroditopic receptors **3** and **4** were also investigated toward a series of dimethylviologen

(paraquat) salts.[30] Due to the very low solubility of paraquat salts in halogenated solvents, preliminary binding studies were accomplished in the gas phase using ESI mass spectrometry.[31]

Gas-phase studies. Samples for mass analysis were prepared by suspending an excess of the solid paraquat salt PQX_2 (X = TsO, Cl, and I) in a refluxing $CHCl_3$ solution of the receptor (~10^{-3} M). After filtration and dilution with methanol (see Experimental), the resulting mixtures were submitted to ESI-MS in the positive mode. Fig. 8a shows the mass spectrum of the mixture of **3** with $PQ(TsO)_2$. The peak at m/z = 806.0 was ascribed to a doubly charged species in which two calix[4]arene units are associated with a paraquat dication: [$\mathbf{3}_2\supset PQ^{2+}$]. Such a supramolecular adduct also gives rise to a weak singly charged ion [$\mathbf{3}_2\supset PQ(TsO)^+$] at m/z = 1783.2 in which a tosylate anion has been retained. The spectrum also shows two intense peaks at m/z = 449.3 and 1069.5 that correspond to the doubly [$\mathbf{3}\supset PQ^{2+}$] and singly [$\mathbf{3}_2\supset PQ(TsO)^+$] charged 1:1 adducts.

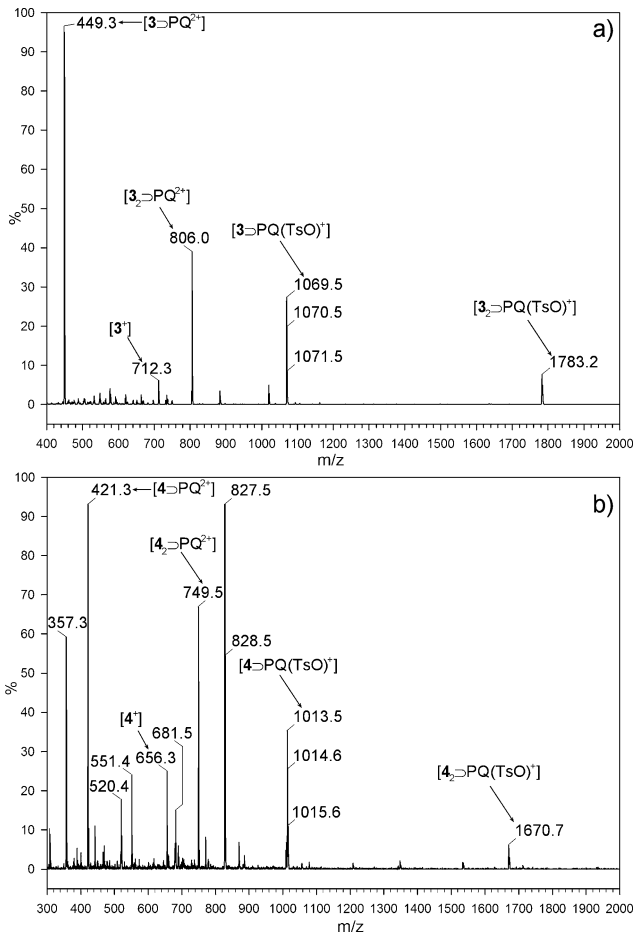

Fig. 8 ESI-MS spectra obtained from the 9:1 $CHCl_3$:MeOH solutions of a) **3** and b) **4** with $PQ(TsO)_2$ (cone voltage: 25–40 V; desolvation temperature: 120 °C).

A similar distribution of ionised species was identified in the mass spectrum of the mixture containing receptor **4** and $PQ(TsO)_2$ (see Fig. 8b). The 2:1 adduct yields peaks at m/z = 749.5 and 1670.7 corresponding to the doubly [$\mathbf{4}_2\supset PQ^{2+}$] and singly [$\mathbf{4}_2\supset PQ(TsO)^+$] charged species, respectively. The 1:1 adduct is recognisable for the intense peaks at m/z = 421.3 [$\mathbf{4}\supset PQ^{2+}$] and 1013.5 [$\mathbf{4}\supset PQ(TsO)^+$]. The two spectra in Fig. 8 also reveal the presence in the gas-phase of the free receptor (m/z = 712.3 and 656.3 for **3** and **4**, respectively). The analysis of the mass spectra recorded in the same experimental conditions from the samples derived by the suspension of $PQCl_2$ and PQI_2 in the solutions of **3** and **4** did not indicate any appreciable formation of supramolecular adduct in the gas-phase.

Solution studies. The formation of the supramolecular adducts between $PQ(TsO)_2$ and receptors **3** and **4** was also studied in low polarity solvents using both NMR and UV/vis spectroscopy. Samples appropriate for NMR analysis were obtained by suspending for 30 min an excess of the solid $PQ(TsO)_2$ in a refluxing $CDCl_3$ solution of each receptor (~2×10^{-2} M). The ^{1}H NMR spectra of the pale yellow solutions obtained after the filtration of the undissolved material showed that both receptors were able to dissolve the paraquat salt in chloroform. The stack plot of Fig. 9 shows that, upon complexation, the resonances of **4** underwent a significant rearrangement (see Fig. 9a). In particular, the large downfield shift (up to 2.6 ppm) experienced by the NH protons of the phenylurea group (*cf.* Fig 9b) is in agreement with a complexation reaction that involves hydrogen bonding with the two tosylate anions. 2D HH COSY and 2D HC HMQC correlation experiments (see ESI†) assigned the doublets resonating at δ = 6.65 (★) and 8.35 (●) ppm to the protons in the *ortho* and *meta* position of the pyridinic rings, respectively. The former of these doublets is noticeably upfield-shifted (~2.3 ppm) with respect to its usual chemical shift in D_2O (see Experimental). An even more marked upfield shift (~3.8 ppm) was observed for the six viologen methyl protons (◆) which resonate, as a singlet, at δ = 0.57 ppm.

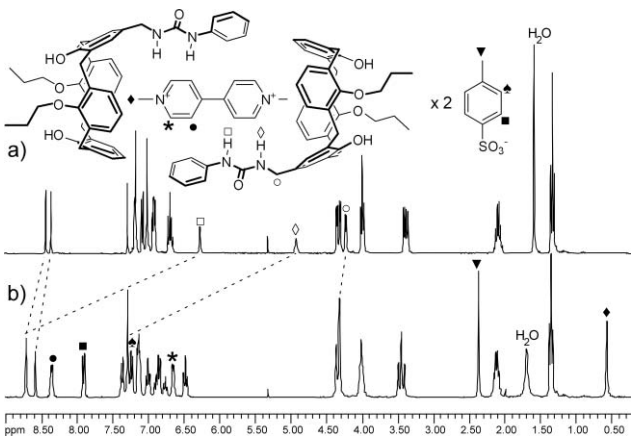

Fig. 9 ^{1}H NMR spectra (300 MHz, $CDCl_3$) of a) **4** and b) its 2:1 complex with $PQ(TsO)_2$. The most representative resonances are indicated with symbols (see sketch).

Considering that the signal integration yields a 2:1 ratio between **4** and $PQ(TsO)_2$, these upfield shifts are likely due to the complexation of the bypyridinium dication within an extended aromatic cavity created by the cooperation of two self-assembled cavities of **4**. 2D ROESY experiments (see ESI†) finally confirmed the spatial close proximity between the methyl protons of the viologen unit with the aromatic protons present on the upper rim of the calix[4]arene macrocycle. The solid-liquid extraction

experiment carried out using the more rigid receptor **3** afforded very similar results (see ESI†).

NMR diffusion experiments (DOSY)[32,33] were then carried out to provide further information on the composition of the $CDCl_3$ solution containing the $\mathbf{4}_2\supset PQ(TsO)_2$ complex (see Experimental). The linear fitting of the attenuation profiles of all the resonances of the spectrum reported in Fig. 9a yielded a mean diffusion coefficient $D = 4.7 \pm 0.1 \times 10^{-6}$ cm^2 s^{-1} (see ESI†). For reference, the diffusion experiment was also performed on the solution of **4**. The calculated diffusion coefficient for the free receptor was $D = 6.8 \pm 0.2 \times 10^{-6}$ cm^2 s^{-1}. This confirms, as expected, that the cumbersome 2:1 supramolecular adduct is a slower diffusing species in solution than the free receptor.¶

The $PQ(TsO)_2$ salt experiences sufficient solubility in neat chloroform to allow a determination through UV/vis spectroscopy of the thermodynamic stability of these 2:1 adducts. Typically, a solution of $PQ(TsO)_2$ salt (1×10^{-5} M) in $CHCl_3$ was titrated with a solution of the receptors (1×10^{-4} M) in $CHCl_3$. The free $PQ(TsO)_2$ yields a main absorption band centred at $\lambda = 272$ nm ($\varepsilon = 2.01 \times 10^4$ mol^{-1} L cm^{-1}) that upon complexation with either **3** or **4** experiences a weak bathochromic shift. The collected spectra were fitted with Specfit/32[27] using the following binding modes:

$$R + PQ \rightleftharpoons^{K_{11}} R \supset PQ \quad (1)$$

$$R \supset PQ + R \rightleftharpoons^{K_{21}} R_2 \supset PQ \quad (2)$$

$$2R + PQ \rightleftharpoons^{\beta_{21}} R_2 \supset PQ \quad (3)$$

where R is the calix[4]arene receptor and PQ is the viologen ion pair. Good fittings were obtained by applying a 2:1 binding mode (eqn. 3) yielding a $\log\beta_{21}$ of 10.2 ± 0.2 and 10.7 ± 0.5 for **3** and **4**, respectively. The UV/vis studies did not reveal the presence in solution of concomitant 1:1 and 2:1 adducts (eqn. 1 and 2).

Solid-state studies. We were able to separate from the chloroform solution crystals of $\mathbf{4}_2\supset PQ(TsO)_2$ suitable for X-ray analysis. The complex is effectively characterised by a "cage" structure with the PQ dication encapsulated within the intramolecular cavity created by the two calix[4]arene units of **4** (see Fig. 10). The mutual attraction between the calixarene cage and the PQ dication occurs through four CH–π interactions involving the hydrogen atoms of the two PQ methyl groups and the four aromatic rings of the calix[4]arene cage (see Table 4 for the geometric parameters of the CH-π interactions).

The conformation of the two calixarene units is quite different one from the other as shown by the conformational parameters ϕ and χ (see ESI†).[28] Such conformation is induced by intramolecular hydrogen bonding O···O contacts between the following phenolic oxygens: O(1A)···O(1D) 2.718(6), O(1C)···O(1D) 2.672(6), O(1C)···O(1B) 2.967(6) Å in the ABCD calixarene, and O(1E)···O(1H) 2.702(6), O(1F)···O(1G) 2.642(6), O(1G)···O(1H) 2.950(6) Å in the EFGH calixarene. In this complex, the strength of the four CH–π interactions is close to the one observed in the $\mathbf{3}_2\supset$NMPCl complex[9] (the C···Ct separations range from 3.164(7) to 3.419(7) Å in $\mathbf{4}_2\supset PQ(TsO)_2$ and from 3.204(1) to 3.535(1) Å in $\mathbf{3}_2\supset$NMPCl). The two tosylate counteranions are located on the border of the cage in close proximity to the PQ dication. Each of them is linked to the urea chain of a calixarene through two strong hydrogen bonds (see Table 4). In such a way all the complex is stabilised by the simultaneous cooperation of three different types of interactions: the coulombic forces (strong but not directional and thus not selective) between the two tosylate anions and the PQ dication; the four hydrogen bonds (directional and selective) which link the two anions to the calixarene cage; the four CH–π interactions (directional and thus selective) which stabilizes the PQ dication within the cage.

Table 4 Geometric parameters relative to the CH–π and hydrogen bonding interactions found in the $\mathbf{4}_2\supset PQ(TsO)_2$ complex.[a]

	Interaction	Distance (Å)		Angle (°)
Entry	Donor–H···Acceptor	H···A	D···A	D–H···A
1	N(1A)–H···O(1I)	2.953	2.014(6)	166
2	N(2A)–H···O(2I)	2.940	2.018(5)	161
3	N(1E)–H···O(3M)	2.936	1.977(5)	177
4	N(2E)–H···O(2M)	3.055	2.104(6)	170
5	C(13)–H··· Ct(A)	2.530	3.419(7)	155
6	C(13)–H···Ct(D)	2.584	3.363(6)	128
7	C(14)–H···Ct(E)	2.814	3.164(7)	127
8	C(14)–H···Ct(F)	2.485	2.014(6)	166

[a] Ct indicates the centroids of the calix[4]arene aromatic rings.

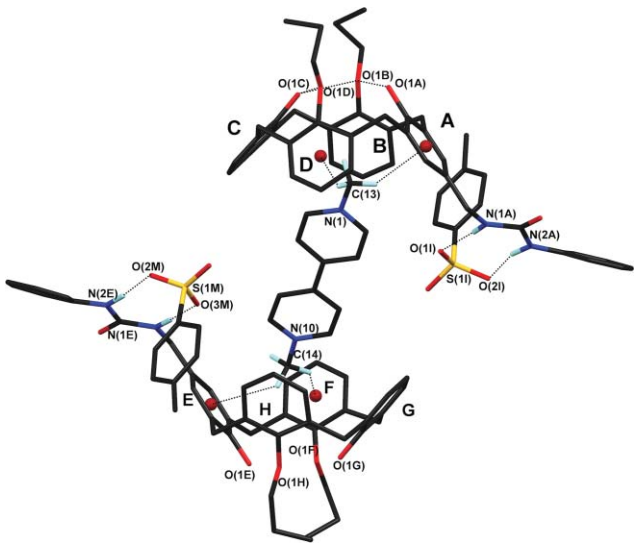

Fig. 10 Perspective stick view of the 2:1 complex $\mathbf{4}_2\supset PQ(TsO)_2$. Several atoms not involved in intermolecular interactions have been omitted for clarity.

Conclusions

The present systematic study shows that, in low polarity media, the binding efficiency of synthetic monotopic calix[4]arene receptors **1** and **2** toward *N*-methylpyridinium salts is strongly dependent on the nature of the anion. In particular, ion-pair binding is prompted by low coordinating anions such as triflimide. On the

¶ The application of the Stokes–Einstein equation $D = k_B T/(c\pi\eta r_H)$, where k_B is the Boltzmann constant, T is the temperature, c is a numerical factor correlated with the size of the diffusing species, and η is the solvent viscosity, yielded, assuming a spherical shape of the diffusing species and using the slip conditions ($c = 4$), a hydrodynamic radius r_H of ~1.2 and ~0.8 nm for the 2:1 complex and the free **4**, respectively.

other hand the ancillary H-bond donor group present on the calixarene scaffold of the heteroditopic receptors **3** and **4** induces a general enhancement of the binding efficiency. The binding data also evidence that the structure of the ion pairs having an anisotropic charge distribution strongly affects the recognition process in particular with the heteroditopic receptors. The large affinity evidenced by the latter receptors for the pyridinium ring was exploited for the complexation of dimethylviologen salts (paraquat). Differently from the *N*-methylpyridinium cation, the paraquat dication (PQ^{2+}) benefits from peculiar redox properties, and its salts could be exploited as an electrochemical switchable "supramolecular bridge" between two calix[4]arene units. The formation of the 2:1 host–guest complexes could be seen as the starting point for the preparation of supramolecular polymers that are switchable by external electrochemical stimuli.

Experimental

Materials and instrumentation

All reactions were carried out under nitrogen; all solvents were freshly distilled under nitrogen and stored over molecular sieves for at least 3 h prior to use. ^{1}H and ^{13}C NMR spectra were recorded on instruments operating at 300 and 75 MHz, respectively. Melting points are uncorrected. Compounds **1**,[20] **2**,[20] **3**,[24] **4**,[25] and *N*-methylpyridinium triflimide[34] ($NMPTf_2N$) were synthesised according to reported procedures. All other reagents were of reagent-grade quality as obtained from commercial suppliers and were used without further purification.

General procedure for the synthesis of NMPX salts. Pyridine (2.3 g, 29 mmol) and the appropriate amount of methylating agent CH_3X (24 mmol) were dissolved in acetonitrile (150 ml). The resulting homogeneous solution was refluxed for 24 h. After cooling to room temperature, 150 mL of ethyl acetate were slowly added to the reaction mixture until a crystalline solid precipitated from the solution. The solid was recovered by suction filtration, washed with ethyl acetate (3 × 25 ml) and dried under vacuum. The recovered salt did not required further purification.

- *N*-Methylpyridinium tosylate (NMPTsO) toluene-4-sulfonic acid methyl ester (4.5 g) was used as methylating agent to afford 5.9 g of NMPTsO as a white solid (92%). M.p.: 138–139 °C; lit: 138–139 °C.[35]
- *N*-Methylpyridinium iodide (NMPI): iodomethane (3.4 g) was used as methylating agent to afford 5.1 g of NMPI as a white solid (96%). M.p.: 117–119 °C; lit: 116–118 °C.[36]
- *N*-Methylpyridinium chloride (NMPCl): The salt was obtained from the corresponding tosylate (NMPTsO) by anion exchange on a 'Dowex' 1-X8 (Cl) 100–200 mesh standard grade resin. The resin (10 g) was initially activated with a solution of HCl (100 ml, 10% w/v in water), treated with a saturated solution of NaCl in water (100 ml), and washed with 200 ml of water. A solution of NMPTsO (2 g, 7.5 mmol) in 10 ml of water was eluted trough the resin. The exchanged product was recovered by washing the resin with 150 ml of water. The solution was dried under vacuum to obtain 0.95 g of NMPCl as a white hygroscopic solid (97%). M.p.: 149–150 °C; lit: 149.5 ± 0.5 °C.[37]
- *N*-Methylpyridinium trifluoroacetate (NMPTFA): a 0.3 M solution of silver trifluoroacetate in water (50 ml) was added to a stirred solution of NMPI (3.3 g, 15 mmol) in 50 ml of water. The resulting solution was filtered off to remove the precipitate of AgI and evaporated to dryness under reduced pressure to afford 2.9 g of NMPTFA as a colourless viscous oil (96%). ^{1}H NMR (DMSO-d_6, 300 MHz) δ (ppm) 9.13 (bd, 2 H, J = 6 Hz), 8.59 (bt, 1 H, J = 6 Hz), 8.14 (bt, 2 H, J = 6 Hz), 4.42 (s, 3 H); ^{13}C NMR (DMSO-d_6, 75 MHz) δ (ppm) 158.3 (q, CF_3C=O, J = 30 Hz), 145.5, 144.8, 127.4, 117.1 (q, CF_3, J = 300 Hz), 47.5. Elemental analysis calculated for $C_8H_8F_3NO_2$: C, 46.38; H, 3.89; N, 6.76%; found: C, 46.43; H, 3.99; N, 6.54%.

General procedure for the synthesis of PQX_2 salts. 4,4′-Bipyridine (2.5 g, 16 mmol) and the appropriate amount of methylating agent CH_3X (40 mmol) were dissolved in acetonitrile (150 ml). The resulting homogeneous solution was refluxed for 24 h. After cooling to room temperature, 150 ml of ethyl acetate were slowly added to the reaction mixture until a crystalline solid precipitated from the solution. The solid was recovered by suction filtration, washed with ethyl acetate (3 × 25 ml) and dried under vacuum. The recovered salt did not require further purification.

- *N*,*N*′-Dimethylviologen ditosylate ($PQ(TsO)_2$): toluene-4-sulfonic acid methyl ester (7.4 g) was used as methylating agent to afford 7.5 g of $PQ(TsO)_2$ as a yellow solid (94%). M.p.: 222–223 °C; ^{1}H NMR (D_2O, 300 MHz) δ (ppm) 8.93 (d, 4 H, J = 6 Hz), 8.35 (d, 4 H, J = 6 Hz), 7.56 (d, 4 H, J = 6 Hz), 7.24 (d, 4 H, J = 6 Hz), 4.43 (s, 6 H), 2.30 (s, 6 H); ^{13}C NMR (D_2O, 75 MHz) δ (ppm) 152.5, 149.4, 145.5, 142.8, 132.6, 129.7, 128.6, 51.5, 23.7. Elemental analysis calculated for $C_{26}H_{28}N_2O_6S_2$: C, 59.07; H, 5.34; N, 5.30; S, 12.13; found: C 59.14%, H 5.40%, N 5.31%, S 12.22%.
- *N*,*N*′-Dimethylviologen diiodide (PQI_2): iodomethane (5.7 g) was used as methylating agent to afford 6.2 g of PQI_2 as a red solid (95%). M.p.: 325–326 °C; lit: 325 °C.[38]

Binding studies

^{1}H NMR continuous variation methods (Job plot). Aliquots of stock solutions in $CDCl_3$ of the receptor (**1–4**) and of the NMPX salt were added to several 5 mm NMR tubes in different ratios maintaining the total molar concentration constant. In this way were prepared 14 samples in which the mole fraction (x) of the interacting species was continuously varied from 0.1 to 1. A ^{1}H NMR spectrum was recorded for each sample. The corresponding Job plot was obtained plotting a property proportional to the complex concentration, in this case $(\delta_{obs} - \delta_{free}) \times [NMPX]_0$, *versus* the mole fraction of the salt. δ_{obs} and δ_{free} represent the chemical shift (ppm) of a resonance of the NMP cation in the complex and in the free salt, respectively. $[NMPX]_0$ is the total concentration of the salt in each tube. The stoichiometry of binding is obtained from the value of the mole fraction on the abscissa that yields the maximum of the plot. For x = 0.5, the stoichiometry of binding is 1:1.

^{1}H NMR titrations. Solutions (500 µl) of the NMPX salts in $CDCl_3$ (c = 1–1.5 × 10^{-3} M) were prepared in a 5 mm NMR tube and small aliquots of a tenfold concentrated solution of the receptor in $CDCl_3$ were added. A ^{1}H NMR spectrum was recorded after each addition. Considering a 1:1 host–guest binding equilibrium, the apparent binding constant is expressed by the following equation:

$$R + S \underset{}{\overset{k}{\rightleftharpoons}} RS \quad K = \frac{[RS]}{[R][S]}$$

where [R], [S], and [RS] are the concentrations of the calix[4]arene receptor, of the NMPX salt and of the complex at the equilibrium, respectively. The binding constants K were calculated through the non-linear fitting of the chemical shift variation of the protons of the NMPX salt using the equation devised by Wilcox:[18]

$$\delta_{obs} = \delta_s + \frac{\Delta\delta}{2[S]_0}\left[\frac{1}{K} + [R]_0 + [S]_0 - \sqrt{\left(\frac{1}{K} + [R]_0 + [S]_0\right)^2 - 4[R]_0[S]_0}\right]$$

$$\Delta\delta = \delta_{RS} - \delta_S$$

where δ_{obs}, δ_S, δ_{RS}, $[R]_0$, and $[S]_0$ are the observed chemical shift of the proton under investigation under fast exchange conditions, the chemical shift of same proton in the free salt and in the complex (guessed), the initial concentration of the guest and of the host, respectively. The conditions of the Weber parameter p ([conc. of the complex]/[maximum possible conc. of the complex]) were verified for each titration experiment according to the calculated binding constant.[18] If necessary the concentrations of the two reactants were adjusted and the NMR titration experiment repeated to explore the proper p range (0.2–0.8).

UV/vis titrations. Spectroscopic titrations were carried out in a quartz cuvette (path length = 1 cm), maintained at 300 K through an external thermostat, by adding small aliquots of a chloroform solution ($c = 2 \times 10^{-4}$ M) of the receptor to a chloroform solution ($c = 2 \times 10^{-5}$ M) of the NMPX salt. The spectral data were collected in the 265–650 nm wavelength range. The binding constants were calculated selecting different binding models with the Specfit/32 software.[27] The fitting of the spectral data was carried out considering the optical variation in the sampled wavelength range. As for the NMR titrations, the Weber parameter p was checked against the calculated binding constant.

ESI-MS measurements. Samples for mass analysis were prepared by suspending a large excess of the solid paraquat salt PQX_2 (X = TsO, Cl, and I) in a 10^{-3} M solution of each receptor (**3** and **4**) in $CHCl_3$. The resulting heterogeneous mixtures were refluxed for at least half an hour, then cooled at room temperature and filtered to remove the undissolved solid material. The recovered homogeneous solutions were then diluted with one-tenth of the volume of methanol and submitted to ESI-MS analysis in the positive mode with a Waters Acquity SQD equipment (cone voltage range: 25–40 V; desolvation temperature: 120 °C).

NMR diffusion experiments. DOSY experiments were carried out in $CDCl_3$ at 300 K on a Bruker Avance 300 Spectrometer using a stimulated echo sequence with bipolar gradients (STEbp).[39] The diffusion coefficient D of the species present in solution was determined by monitoring the intensity decay of at least six resonances present in the NMR spectrum of the sample as a function of gradient strength applied to the sample. The fitting of the attenuation profiles was carried out using the equation:

$$I = I_0 \exp\left(-D\gamma^2 g^2 \delta^2 \left(\Delta - \frac{\delta}{3} - \frac{\tau}{2}\right)\right)$$

Table 5 Crystal data for **1**⊃NMPI and **4**$_2$⊃$PQ(TsO)_2$

	1⊃NMPI	**4**$_2$⊃$PQ(TsO)_2$
Empirical formula	$C_{36}H_{36}O_6 \cdot C_6H_8NI$	$2C_{42}H_{44}N_2O_5 \cdot C_{12}H_{14}N_2 \cdot 2C_7H_7SO_3$
Formula weight	785.717	1842.277
Crystal system	Trigonal	Monoclinic
Space group	$P3_1$ (no. 144)	$P2_1$ (no. 4)
a (Å)	18.564(1)	11.284(5)
b (Å)	18.564(1)	14.758(5)
c (Å)	10.127(1)	29.067(5)
α (°)	90	90
β (°)	90	91.04(2)
γ (°)	120	90
V (Å^3)	3022.4(2)	4840(3)
Z	3	2
D_{calc} (g/cm^{-3})	1.295	1.264
$F(000)$	1212	1956
Data collection		
Temperature (K)	293	293
θ Range (°)	3.0–70.0	3.0–70.0
Index ranges	$-22 \le h \le 22$ $-22 \le k \le 20$ $-5 \le l \le 12$	$-13 \le h \le 13$ $-15 \le k$ 17 $-27 \le l \le 35$
Refl. measured	6301	9717
Indep. reflections	4635 (R_{int} = 0.069)	9527 (R_{int} = 0.0409)
Obs. refl. $[F_o > 4\,\sigma(F_o)]$	2719	3432
Data/Restr./Param.	2719/14/452	3432/33/1077
Structure refinement		
Final R indices[a] (obs. data)	R1= 0.0584 $wR2$= 0.092	$R1$ = 0.073 $wR2$ = 0.2062
Goodness of fit S[b]	0.925	0.95
Min. and max. residual ρ (e/Å^3)	0.34, –0.54	0.32, –0.25

[a] $R1 = \Sigma\,||F_o| - |F_c|| \,/\, \Sigma\,|F_o|$, $wR2 = [\Sigma\, w(F_o^2 - F_c^2)^2 \,/\, \Sigma wF_o^4]^{1/2}$. [b] Goodness-of-fit $S = [\Sigma\, w(F_o^2 - F_c^2)^2 \,/\, (n-p)]^{1/2}$, where n is the number of reflections and p the number of parameters.

where I is the intensity of the observed resonance (attenuated), I_0 the intensity of the reference resonance (unattenuated), D the diffusion coefficient, γ the gyromagnetic ratio, g the gradient strength, δ the gradient pulse length, Δ the diffusion time, and τ the dephasing and rephasing correction time. For each sample 16 experiments were carried out, in which the gradient strength g was varied from 5 to 95% of the maximum gradient intensity (5.35 G/mm).

X-ray crystallographic analysis. Crystallographic data for **1**⊃NMPI and **4**$_2$⊃$PQ(TsO)_2$ are summarised in Table 5.† Intensity data were collected on a Enraf-Nonius CAD4 diffractometer equipped with a CuKα radiation source (λ = 1.54178 Å). The structures were solved by direct methods using SIR2004[40] and refined on F^2 by full-matrix least-squares methods, using SHELXL-97.[41] All the non-hydrogen atoms were refined with anisotropic atomic displacements. For the **1**⊃NMPI structure, the hydrogen atoms were included in the refinement at idealised geometries and refined "riding" on the corresponding parent atoms with common isotropic atomic displacements 1.2 times those of their parent atoms. The structure of **1**⊃NMPI has a pseudo two-fold symmetry and can be refined both in the $P3_1$ space group, where the **1**⊃NMPI complex has a C_1 symmetry, and in the $P3_121$ space group, where both the calixarene and the N-methylpyridinium guest have a crystallographically imposed two-fold symmetry with

the three guest methyl hydrogen atoms disordered over two different orientations. We were intrigued in the choice between the two space groups, however the comparison between the refinements in the two space groups showed that: a) the final electron density difference ΔF map in the $P3_1$ space group did not show residual peaks to support the hypothesis of the disordered guest methyl group; b) the refinement in the $P3_121$ space group converged at a higher $R1$ value (0.0616). On these basis we concluded that the correct space group is $P3_1$with a pseudo-C_2 symmetry. In the $\mathbf{4}_2 \supset PQ(TsO)_2$ structure, systematic $h0l$ absences clearly indicate the $P2_1$ space group even if the structure approximates a $P2_1/c$ space group. The hydrogen atoms were placed at their calculated positions with the geometric constraint C–H 0.96 Å and refined "riding" on their corresponding carbon atoms with relative isotropic atomic displacements. Geometric calculations were performed with the PARST97[42].

Acknowledgements

This work was partly supported by the Italian MIUR (Sistemi Supramolecolari per la Costruzione di Macchine Molecolari, Conversione dell'Energia, Sensing e Catalisi). We thank CIM (Centro Interdipartimentale di Misure), G. Casnati of the University of Parma for NMR measurements and Dr. Stefano Sforza of the University of Parma for a fruitful discussion on mass measurements.

References

1 (*a*) V. Balzani, A. Credi and M. Venturi, *Molecular Devices and Machines*, Wiley-VCH, Weinheim, 2003; (*b*) V. Balzani, *Small*, 2005, **1**, 278–283.
2 See, for example, *Core Concepts in Supramolecular Chemistry and Nanochemistry*, eds. J. W. Steed, D. R. Turner and K. J. Wallace, John Wiley & Sons, Chichester, 2007.
3 (*a*) *Calixarenes 2001*, eds. Z. Asfari, V. Böhmer, J. Harrowfield and J. Vicens, Kluwer Academic Publishers, Dordrecht, 2001; (*b*) *Calixarenes in the Nanoworld*, eds. J. Harrowfield and J. Vicens, Dordrecht, 2007.
4 For recent papers on ion-pair binding with calixarene-based receptors, see, for example: (*a*) D. E. Gross, F. P. Schmidtchen, W. Antonius, P. A. Gale, V. M. Lynch and J. L. Sessler, *Chem. Eur. J.*, 2008, **14**, 7822–7827; (*b*) M. Hamon, M. Menand, S. Le Gac, M. Luhmer, V. Dalla and I. Jabin, *J. Org. Chem.*, 2008, **73**, 7067–7071; (*c*) M. D. Lankshear, I. M. Dudley, K. M. Chan, A. R. Cowley, S. M. Santos, V. Felix and P. D. Beer, *Chem. Eur. J.*, 2008, **14**, 2248–2263; (*d*) S. Le Gac and I. Jabin, *Chem. Eur. J.*, 2008, **14**, 548–557; (*e*) M. D. Lankshear, N. H. Evans, S. R. Bayly and P. D. Beer, *Chem. Eur. J.*, 2007, **13**, 3861–3870; (*f*) M. Cametti, M. Nissinen, A. Dalla Cort, L. Mandolini and K. Rissanen, *J. Am. Chem. Soc.*, 2007, **129**, 3641–3648; (*g*) V. Felix, M. G. Drew, P. R. Webber and P. D. Beer, *Phys. Chem. Chem. Phys.*, 2006, **8**, 521–532; (*h*) J. L. Sessler, D. An, W. S. Cho, V. Lynch and M. Marquez, *Chem. Eur. J.*, 2005, **11**, 2001–2011; (*i*) T. Nabeshima, T. Saiki, J. Iwabuchi and S. Akine, *J. Am. Chem. Soc.*, 2005, **127**, 5507–5511 and references therein.
5 (*a*) A. Arduini, A. Credi, G. Faimani, C. Massera, A. Pochini, A. Secchi, M. Semeraro, S. Silvi and F. Ugozzoli, *Chem. Eur. J.*, 2008, **14**, 98–106; (*b*) A. Credi, S. Dumas, S. Silvi, M. Venturi, A. Arduini, A. Pochini and A. Secchi, *J. Org. Chem.*, 2004, **69**, 5881–5887; (*c*) F. Ugozzoli, C. Massera, A. Arduini, A. Pochini and A. Secchi, *CrystEngComm*, 2004, **6**, 227–232; (*d*) A. Arduini, F. Calzavacca, A. Pochini and A. Secchi, *Chem. Eur. J.*, 2003, **9**, 793–799; (*e*) A. Arduini, R. Ferdani, A. Pochini, A. Secchi and F. Ugozzoli, *Angew. Chem., Int. Ed.*, 2000, **39**, 3453.
6 (*a*) A. Arduini, A. Pochini and A. Secchi, *Eur. J. Org. Chem.*, 2000, 2325–2334; (*b*) A. Arduini, W. M. McGregor, D. Paganuzzi, A. Pochini, A. Secchi, F. Ugozzoli and R. Ungaro, *J. Chem. Soc., Perkin Trans. 2*, 1996, 839.
7 (*a*) A. Arduini, E. Brindani, G. Giorgi, A. Pochini and A. Secchi, *J. Org. Chem.*, 2002, **67**, 6188–6194; (*b*) A. Arduini, G. Giorgi, A. Pochini, A. Secchi and F. Ugozzoli, *J. Org. Chem.*, 2001, **66**, 8302–8308.
8 For recent examples of positive allosteric effect on ion-pair binding, see, for example: (*a*) K. Zhu, S. Li, F. Wang and F. Huang, *J. Org. Chem.*, 2009, **74**, 1322–1328; (*b*) C. M. G. dos Santos, T. McCabe, G. W. Watson, P. E. Kruger and T. Gunnlaugsson, *J. Org. Chem.*, 2008, **73**, 9235–9244; (*c*) J. L. Sessler, E. Tomat and V. M. Lynch, *J. Am. Chem. Soc.*, 2006, **128**, 4184–4185; (*d*) L. Kovbasyuk and R. Kramer, *Chem. Rev.*, 2004, **104**, 3161–3188.
9 L. Pescatori, A. Arduini, A. Pochini, A. Secchi, C. Massera and F. Ugozzoli, *CrystEngComm*, 2009, **11**, 239–241.
10 (*a*) S. Tsuzuki and A. Fujii, *Phys. Chem. Chem. Phys.*, 2008, **10**, 2584–2594; (*b*) M. Nishio and Y. Umezawa, in *Topics in Stereochemistry*, eds. S. E. Denmark and J. S. Siegel, John Wiley & Sons, Hoboken, NJ, 2006, vol. 25, pp. 255–302.; (*c*) M. Nishio, *CrystEngComm*, 2004, **6**, 130.
11 (*a*) N. Zacharias and D. A. Dougherty, *Trends Pharmacol. Sci.*, 2002, **23**, 281–287; (*b*) J. P. Gallivan and D. A. Dougherty, *Proc. Natl. Acad. Sci. U. S. A.*, 1999, **96**, 9459; (*c*) J. C. Ma and D. A. Dougherty, *Chem. Rev.*, 1997, **97**, 1303–1324.
12 (*a*) *Intelligent Materials*, eds. M. Shahinpoor and H.-J. Schneider, Royal Society of Chemistry, Cambridge, 2007; (*b*) *Supramolecular Polymers*, ed. A. Ciferri, Marcel-Dekker, New York, 2000; (*c*) C. Rao, *Supramolecular Organization and Materials Design*, Cambridge University Press, 2001.
13 For the recognition of *N*-alkyl pyridinium and *N*,*N*′-dialkyl dipyridinium salts by calix[*n*]arene derivatives in aqueous media, see, for example: (*a*) R. Kaliappan, Y. Ling, A. E. Kaifer and V. Ramamurthy, *Langmuir*, 2009, DOI: 10.1021/la900659r; (*b*) D.-S. Guo, K. Wang and Y. Lu, *J. Inclusion Phenom. Macrocyclic Chem.*, 2008, **62**, 1; (*c*) C. Gaeta, T. Caruso, M. Mincolelli, F. Troisi, E. Vasca and P. Neri, *Tetrahedron*, 2008, **64**, 5370–5378; (*d*) N. Korbakov, P. Timmerman, N. Lidich, B. Urbach, A. Sa′ar and S. Yitzchaik, *Langmuir*, 2008, **24**, 2580–2587; (*e*) D.-S Guo, L.-H. Wang and Y. Liu, *J. Org. Chem.*, 2007, **72**, 7775–7778; (*f*) T. R. Tshikhudo, D. Demuru, Z. Wang, M. Brust, A. Secchi, A. Arduini and A. Pochini, *Angew. Chem., Int. Ed.*, 2005, **44**, 2913.
14 For a review on determination of binding constants using NMR data, see: L. Fielding, *Tetrahedron*, 2000, **56**, 6151–6170.
15 The interaction of the counterion with cations or anions in apolar organic solvents is mainly electrostatic in nature, but other contributions may not be neglected. The evaluation of such interaction becomes problematic when cations, such as the planar *N*-alkylpyridinium, characterised both by non-isotropic charge distribution and important stereoelectronic requirements are present in the pair. To the best of our knowledge, there are only few systematic evaluation of the interacting power of anions in ion pairing, see, for example: (*a*) K. Fumino, A. Wulf and R. Ludwig, *Angew. Chem., Int. Ed.*, 2008, **47**, 3830; (*b*) R. Bini, O. Bortolini, C. Chiappe, D. Pieraccini and T. Siciliano, *J. Phys. Chem. B*, 2007, **111**, 598–604.
16 The study of the interaction energy of tetramethylammonium ion pairs having different counteranions with a host with low steric hindrance can be employed as an additional experimental method to evaluate such interactions, see , for example: (*a*) S. Bartoli and S. Roelens, *J. Am. Chem. Soc.*, 2002, **124**, 8307–8315; (*b*) V. Böhmer, A. Dalla Cort and L. Mandolini, *J. Org. Chem.*, 2001, **66**, 1900–1902and Ref. 7a.
17 K. A. Connors, *Binding Constants*, Wiley, New York, 1987.
18 C. S. Wilcox, in *Frontiers of Supramolecular Organic Chemistry and Photochemistry*, eds. H.-J. Schneider and H. Dürr, VCH, Weinheim, 1991, pp. 123–143.
19 The interaction of **1** with NMPCl and NMPI salts can be complicated by the partial dissociation of the ion pairs that add further binding equilibria to the 1:1 binding model. These effects and their mathematical treatment have been very recently discussed by Roelens and co-workers; see: S. Roelens, A. Vacca and F. Venturi, *Chem. Eur. J.*, 2009, **15**, 2635–2644.
20 A. Arduini, M. Fabbi, M. Mantovani, L. Mirone, A. Pochini, A. Secchi and R. Ungaro, *J. Org. Chem.*, 1995, **60**, 1454–1457.
21 G. Arena, A. Contino, E. Longo, G. Spoto, A. Arduini, A. Pochini, A. Secchi, C. Massera and F. Ugozzoli, *New J. Chem.*, 2004, **28**, 56.
22 See *e. g.* S. Grimme, *Angew. Chem., Int. Ed.*, 2008, **47**, 3430 and references therein.
23 (*a*) Despite the residual conformational flexibility, **2** still possesses an aromatic cavity more preorganized than the corresponding tetra-*O*-alkylated calix[4]arene derivatives as theoretically predicted and experimentally verified for *O*-methylated calix[4]arene derivatives; see:

W. P. van Hoorn, M. G. H. Morshuis, F. C. J. M. van Veggel and D. N. Reinhoudt, *J. Phys. Chem. A*, 1998, **102**, 1130–1138; (*b*) T. Kusano, M. Tabatabai, Y. Okamoto and V. Böhmer, *J. Am. Chem. Soc.*, 1999, **121**, 3789–3790.
24 A. Arduini, A. Secchi and A. Pochini, *J. Org. Chem.*, 2000, **65**, 9085–9091.
25 A. Arduini, E. Brindani, G. Giorgi, A. Pochini and A. Secchi, *Tetrahedron*, 2003, **59**, 7587–7594.
26 J. S. Brinen, J. G. Koren, H. D. Olmstead and R. C. Hirt, *J. Phys. Chem.*, 1965, **69**, 3791–3794.
27 SPECFIT/32™ Global Analysis System for Windows.
28 F. Ugozzoli and G. D. Andreetti, *J. Inclusion Phenom. Mol. Recognit. Chem.*, 1992, **13**, 337.
29 *Handbook of Chemistry and Physics*, 76th edition, CRC Press, 1996.
30 P. M. Monk, *The Viologens*, John Wiley & Sons, Chichester, 1998.
31 For a review on the use of mass technique for the evaluation of binding in the gas-phase, see: M. Kogey and C. A. Schalley in *Analytical Methods in Supramolecular Chemistry*, ed. C. A. Schalley, Wiley-VCH, Weinheim, 2007, pp. 104–162.
32 C. S. Johnson, *Prog. Nucl. Magn. Reson. Spectrosc.*, 1999, **34**, 203–256 and references therein.
33 For a general review on the application of DOSY in supramolecular chemistry, please see: Y. Cohen, L. Avram and L. Frish, *Angew. Chem., Int. Ed.*, 2005, **44**, 520.
34 Y. Nakamura, T. Maki, X. Wang, K. Ishihara and H. Yamamoto, *Adv. Synth. Catal.*, 2006, **348**, 1505–1510.
35 C. S. Marvel, E. W. Scott and K. L. Amstutz, *J. Am. Chem. Soc.*, 1929, **51**, 3638–3641.
36 J. R. Ames, *J. Pharm. Sci.*, 1991, **80**, 293–295.
37 D. S. Newman, D. P. Morgan and R. T. Tiliack, *J. Chem. Eng. Data*, 1976, **21**, 279–281.
38 J. H. Ross and R. I. Krieger, *J. Agric. Food Chem.*, 1980, **28**, 1026–1031.
39 D. Wu, A. Chen and C. S. Johnson, Jr., *J. Magn. Reson.*, 1995, **A115**, 123.
40 SIR2004M. C. Burla, R. Caliandro, M. Camalli, B. Carrozzini, G. L. Cascarano, L. De Caro, C. Giacovazzo, G. Polidori and R. Spagna, *J. Appl. Crystallogr.*, 2005, **38**, 381.
41 G. M. Sheldrick, *SHELXL97, program for crystal structure refinement*, University of Göttingen, Germany, 1997, http://shelx.uni-ac.gwdg.de/shelx/index.html.
42 M. Nardelli, *J. Appl. Crystallogr.*, 1996, **29**, 296–300.

